journal

J. Am. Ceram. Soc., 76 [6] 1595–601 (1993)

Phase Relations in the System Al_2O_3–$Ce_2Si_2O_7$ in the Temperature Range 900° to 1925°C in Inert Atmosphere

A. Cuneyt Tas* and Mufit Akinc*

Department of Materials Science and Engineering, Iowa State University, Ames, Iowa 50011

Equilibrium relationships in the system Al_2O_3–$Ce_2Si_2O_7$ in inert atmosphere have been investigated in the temperature range 900° to 1925°C. A simple eutectic reaction was found at 1375°C and 51 mol% $Ce_2Si_2O_7$. A high–low polymorphic transformation in $Ce_2Si_2O_7$ was observed at 1274°C. New XRD patterns are suggested for both polymorphs of cerium pyrosilicate. The melting point of $Ce_2Si_2O_7$ was found to be 1788°C. A value for $\Delta H^{\circ}_{m,Ce2Si2O7}$ of 36.81 kJ/mol was calculated from the initial slope of the experimentally determined liquidus in equilibrium with the pyrosilicate phase.

I. Introduction

The present study is concerned with the phase relations between cerium pyrosilicate (disilicate), $Ce_2Si_2O_7$, and Al_2O_3. $Ce_2Si_2O_7$ has been shown to have two polymorphs, a pseudo-orthorhombic high-temperature[1] and a tetragonal low-temperature form.[2,3] The high-temperature form has been reported first to have an orthorhombic space group of $Pna2_1$ (or $Pnam$) by Felsche and Hirsiger.[4] This space group has later been changed to the monoclinic space group of $P2_1/n$, by Felsche,[1] after very weak reflections $h01$ with $h \neq 2n$ had been observed on overexposed precession photographs. Though Felsche[1] pointed out the significant resemblance of the structure of the high-temperature form of cerium pyrosilicate to that of α-$Ca_2P_2O_7$, which was identified[5] by the lattice constants, a = 12.66 Å, b = 8.542 Å, c = 5.315 Å and a monoclinic angle β = 90.3°, he reported the compound to have a monoclinic angle of 90° and preferred to describe it as pseudo-orthorhombic. The high-to-low transition has been reported to be extremely sluggish.[1,2] The melting point of $Ce_2Si_2O_7$ has been reported to be 1770° ± 25°C.[6] It has been reported[7] that, under strongly oxidizing conditions, the cerium ion remains in the 4+ state (CeO_2) and does not react with SiO_2 to form the pyrosilicate. However, it has also been shown[8] that, when high-purity CeO_2 and fumed SiO_2 are mixed together in stoichiometric pyrosilicate proportions and heated to $T > 1550$°C in air for extended periods, pyrosilicate forms and can be quenched to room temperature, with small amounts of $Ce_{4.67}[SiO_4]_3O$ being present as an impurity phase (the absent SiO_2 either being combined with a glassy phase or having sublimed as SiO). On the other hand, if, instead of quenching, the heated mixture is subjected to slow cooling from 1550° to 1300°C in air, the result is decomposition of the pyrosilicate phase into CeO_2 and α-cristobalite.[8] This necessitates the use of an inert or neutral atmosphere in a study of the high-temperature phase relations of the Ce^{3+} silicates and aluminosilicates. The lack of detailed data in the CeO_2–SiO_2 binary, especially those concerning the thermal stability range of the pyrosilicate phase, makes it appropriate for such a study to begin with the synthesis and characterization of $Ce_2Si_2O_7$.

Very few studies[8–11] have been found in the literature that focus on the synthesis of cerium containing aluminosilicate glasses and crystalline materials. These have commonly been studies at one temperature (1500°–1550°C) and one or two different compositions in the ternary system CeO_2–Al_2O_3–SiO_2 and, hence, were far from being phase equilibria studies in terms of scope. O'Brien and Akinc[8] were the first to report the coexistence in air of the solid phases $Ce_2Si_2O_7$ and Al_2O_3 in a liquid matrix containing CeO_2, SiO_2, and Al_2O_3. This finding provided the impetus for the present study, which is hoped to broaden the understanding of this binary system.

II. Experimental Methods

Compositions in the Al_2O_3–$Ce_2Si_2O_7$ system of specific atomic ratios of Al:Ce:Si were prepared by mixing the appropriate amounts of the oxides CeO_2, Al_2O_3, and SiO_2 under acetone in an agate mortar for approximately 1 h. The chemical analyses, the mean particle sizes, and surface areas of the starting oxides are given in Table I. Chemical analyses were determined using laser source mass spectrometry, particle size analyses using light absorbance (Model CAPA 700, Horiba) and surface area using nitrogen adsorption (Model 4200, Leeds and Northrup). The oxides were heated in air at 975°C for 12 h prior to weighing. The compositions studied are indicated in Table II. For each composition, approximately 2-g samples of the mixture were weighed and uniaxially pressed into 1.27-cm-diameter pellets in a tungsten carbide-lined steel die at about 200 MPa. For compositions close to the end members, the oxide mixtures were cold isostatically pressed at 200 MPa following uniaxial dry pressing at 35 MPa.

The pellets were equilibrated at a predetermined temperature in a $MoSi_2$ quench furnace with a vertical 120-cm-long alumina reaction tube. The inert atmosphere in the furnace tube was maintained by constant flow of either prepurified argon or argon + 10% H_2 gases. The pellets were contained in envelopes made from thin foils of Pt (for Ar) or Mo (for Ar + 10% H_2). At the end of the specified equilibration times, the samples were quenched by dropping into an ice-water bath, covered with a thin layer of vacuum pump oil, which also served to seal the bottom end of the furnace tube. The minimum equilibration time during preliminary experiments was 17 h. After 17 h of heating, the samples were quenched, examined by XRD for phase analysis, re-pelletized, and heated for an additional 17 h followed by quenching and phase analysis. The minimum time required for a certain composition to reach equilibrium at a certain temperature was deduced when XRD traces showed no detectable changes in kinds and amounts of the phases present. The temperature in the furnace tube was controlled to within ±6°C. The temperature in the hot zone was monitored with a B-type thermocouple, which was calibrated after every 120 h of heating against the melting points of Au (1064°C) and Pd (1554°C) under a moderate flow of argon.

For phase analysis, every ground quenched sample was examined using XRD in the 5°–85° 2θ range using a powder

E. R. Kreidler—contributing editor

Manuscript No. 195241. Received October 8, 1992; approved February 17, 1993.

*Member, American Ceramic Society.

Table I. Chemical Analysis of Starting Materials

Oxide	CeO_2*	Fumed SiO_2†	Al_2O_3‡
Al_2O_3	94 ppm	9 ppm	99.96 wt%
SiO_2	235 ppm	99.98 wt%	88 ppm
Na_2O	121 ppm	18 ppm	76 ppm
CeO_2	99.87 wt%		
Fe_2O_3	114 ppm	4 ppm	49 ppm
CaO	112 ppm	59 ppm	30 ppm
MgO	13 ppm	2 ppm	20 ppm
Ga_2O_3	121 ppm	<1 ppm	50 ppm
MnO	10 ppm	<1 ppm	5 ppm
Cr_2O_3	88 ppm	<1 ppm	4 ppm
CuO	25 ppm	<1 ppm	10 ppm
Li_2O	9 ppm	<1 ppm	37 ppm
ZnO	5 ppm	2 ppm	25 ppm
NiO	11 ppm	3 ppm	3 ppm
TiO_2	8 ppm	17 ppm	
Sc_2O_3	15 ppm	15 ppm	
K_2O	24 ppm	7 ppm	
La_2O_3	152 ppm		
Pr_6O_{11}	36 ppm		
Gd_2O_3	12 ppm	6 ppm	
B_2O_3	68 ppm	13 ppm	
C	89 ppm	400 ppm	
Cl^-	20 ppm	33 ppm	
Surface area	6.2 m^2/gm	400 m^2/gm	7.5 m^2/gm
Mean particle size	0.7 μm	0.007 μm	0.4 μm

*Cerac, Inc., Milwaukee, WI, Lot No. 36171-A-1. †Sigma Chemical Company, St. Louis, MO, Lot No. 114F-0070. ‡Reynolds, Inc., Richmond, VA, Lot No. BM-2415.

Table II. Results of Equilibration Runs in the System Al_2O_3–$Ce_2Si_2O_7$

Composition	Temperature (°C)	Time (h)	Phase(s) observed
PYRO 5*	1560	40	Liquid + Al_2O_3
PYRO 10	1560	40	Liquid + Al_2O_3
PYRO 15	1560	40	Liquid + Al_2O_3
PYRO 20	1560	40	Liquid + Al_2O_3
PYRO 30	1560	40	Liquid + Al_2O_3
PYRO 40	1560	40	Liquid
PYRO 44	1560	40	Liquid
PYRO 48	1560	40	Liquid
PYRO 50	1560	40	Liquid
PYRO 51	1560	40	Liquid
PYRO 52	1560	40	Liquid
PYRO 54	1560	40	Liquid
PYRO 56	1560	40	Liquid
PYRO 58	1560	40	Liquid
PYRO 60	1560	40	Liquid
PYRO 70	1560	40	Liquid + *m*-$Ce_2Si_2O_7$
PYRO 75	1560	40	Liquid + *m*-$Ce_2Si_2O_7$
PYRO 80	1560	40	Liquid + *m*-$Ce_2Si_2O_7$
PYRO 85	1560	40	Liquid + *m*-$Ce_2Si_2O_7$
PYRO 90	1560	40	Liquid + *m*-$Ce_2Si_2O_7$
PYRO 95	1560	40	Liquid + *m*-$Ce_2Si_2O_7$
PYRO 100	1560	>7	*m*-$Ce_2Si_2O_7$
PYRO 15	1480	70	Liquid + Al_2O_3
PYRO 30	1480	65	Liquid + Al_2O_3
PYRO 50	1480	50	Liquid
PYRO 70	1480	60	Liquid + *m*-$Ce_2Si_2O_7$
PYRO 90	1480	70	Liquid + *m*-$Ce_2Si_2O_7$
PYRO 15	1400	85	Liquid + Al_2O_3
PYRO 30	1400	75	Liquid + Al_2O_3
PYRO 50	1400	50	Liquid
PYRO 70	1400	65	Liquid + *m*-$Ce_2Si_2O_7$
PYRO 90	1400	75	Liquid + *m*-$Ce_2Si_2O_7$
PYRO 15	1300	120	Al_2O_3 + *m*-$Ce_2Si_2O_7$
PYRO 30	1300	90	Al_2O_3 + *m*-$Ce_2Si_2O_7$
PYRO 50	1300	75	Al_2O_3 + *m*-$Ce_2Si_2O_7$
PYRO 70	1300	80	Al_2O_3 + *m*-$Ce_2Si_2O_7$
PYRO 90	1300	100	Al_2O_3 + *m*-$Ce_2Si_2O_7$
PYRO 30	1560	40	
	1200	96	(Cooling rate: 8°C/h) Al_2O_3 + *t*-$Ce_2Si_2O_7$
PYRO 75	1560	40	
	1200	96	(Cooling rate: 8°C/h) Al_2O_3 + *t*-$Ce_2Si_2O_7$

*PYRO 5: 5 mol% $Ce_2Si_2O_7$–95 mol% Al_2O_3.

diffractometer (XDS 2000, Scintag, Santa Clara, CA) with a maximum scanning rate of 0.4° 2θ/min. Silicon (NBS640a) was used as an external standard. The diffraction patterns given in this study were produced with a scan rate of 0.1° 2θ/min in the same 2θ range. Microstructural analyses were carried out using SEM and reflected light microscopy. The chemical compositions of the microstructural features observed in SEM were examined with EDXS and are believed to be accurate to within ±4 at.%.

Differential thermal analysis (DTA) experiments were carried out to monitor the phase transitions in this system. The DTA runs were performed either in Mo foil crucibles in a tungsten-mesh vacuum furnace (Centorr Associates, Suncook, NH) (P_{O_2} being less than 6×10^{-9} atm) using type C thermocouples or in Pt crucibles in an argon atmosphere in a $MoSi_2$ furnace using type B thermocouples. Two heating rates (3° and 6°C/min) were used for every composition. The thermocouples of the vacuum DTA unit (Oxy-gon Industries, Epsom, NH), Type C, were calibrated against the melting points of Au (1064°C), Li_2SiO_3 (1204°C), Pd (1554°C), and Pt (1772°C). The sample for each DTA run was first equilibrated at 1560°C for 40 h in Ar atmosphere, water-quenched, and then ground to a fine powder, followed by X-ray analysis. For each composition selected for DTA analysis, the first run scanned the whole temperature range (900°–1925°C). Upon reaching the maximum temperature, the furnace contents were quenched to room temperature by shutting off the power to the furnace. The quenched samples were then analyzed by XRD and by SEM. The second run for the same composition (with a fresh, equilibrated powder sample) scanned between 900°C and the temperature at which the first thermal event ended as observed in the initial DTA run. The furnace-quenched second sample was also subjected to XRD analysis to determine the phases present and the nature of that thermal event. The subsequent run, analyzed as before, covered the temperature range between 900°C and the temperature at which the second thermal event commenced (if there was one).

III. Results and Discussion

The high-temperature monoclinic polymorph of $Ce_2Si_2O_7$, with the lattice parameters $a = 13.080$ Å, $b = 8.727$ Å, $c = 5.405$ Å, and $\beta = 90.13°$, was synthesized as a single-phase silicate without any difficulty at 1560°C in argon using a heating rate of 4°C/min to the peak temperature, with a hold for 7 h followed by quenching. For holding times less than 7 h, small amounts of $Ce_{4.67}[SiO_4]_3O$ (cerium oxygen apatite) were found to be present in our samples. Monoclinic $Ce_2Si_2O_7$ could be cooled down to 1350°C at a typical rate of 4°C/min under flowing purified argon; however, below 1350°C, it partially decomposed to $Ce_{4.67}[SiO_4]_3O$. Monoclinic cerium pyrosilicate could be preserved as the stoichiometric phase only when it was cooled down to 900°C in vacuum or in an Ar + 10% H_2 atmosphere.

We hereby present a new XRD pattern (Table III)* for the monoclinic $Ce_2Si_2O_7$ phase. This pattern, although still pointing to a similar-sized unit cell by that given by JCPDS PDF pattern 23-0318, after Felsche and Hirsiger,[4] reveals, for the first time, the monoclinic nature of $Ce_2Si_2O_7$, with a small monoclinic angle of 90.13°, owing to its high resolution. The 135 reflections observed in the 5°–85° 2θ range also showed the characteristic peak splitting that could be seen in a monoclinic structure. The 18 strongest reflections of this pattern were displayed in Table IV of this article. This finding for $Ce_2Si_2O_7$, therefore, warrants the further structural investigation of the high-temperature forms of pyrosilicate phases of the remaining light rare-earth elements, i.e., La, Pr, Nd and Sm, which were reported by Felsche[1] to have similar pseudo-orthorhombic structures with the same space group, $P2_1/n$.

The low-temperature tetragonal polymorph of $Ce_2Si_2O_7$ was synthesized by very slow (4°C/h) cooling of the high-temperature form (monoclinic phase) from 1560° to 1175°C in a purified Ar + 10% H_2 atmosphere followed by 60 h of annealing at 1175°C followed by quenching. Felsche[1] was not able to produce this phase by cooling the monoclinic form from 1550°C at 30°C/h to below 1200°C. We also tried this cooling rate and confirmed Felsche's observation. Heindl *et al.*[2] were the first to synthesize this compound by slow cooling (5°C/h) the high-temperature form, and they found that the lattice parameters of the tetragonal polymorph fall between those of the tetragonal forms of $La_2Si_2O_7$ and $Pr_2Si_2O_7$ in the light lanthanide pyrosilicate series. Very recently, van Hal and Hintzen[3] claimed that they found "a new $Ce_2Si_2O_7$ compound never reported before for cerium silicates" and suggested an XRD pattern for the tetragonal polymorph of $Ce_2Si_2O_7$. van Hal and Hintzen used almost the same starting materials as did Heindl *et al.*,[2] i.e., $Ce(NO_3)_3$ and reactive forms of SiO_2, and both carried out their anneals in a H_2 (7% and 5%, respectively)–N_2 atmosphere. As we have shown[12] in a previous study on another cerium silicate, $Ce_{4.67}[SiO_4]_3O$, this phase is susceptible to taking nitrogen into the structure by substituting for oxygen. Nitrogen can be incorporated into the structure not only from nitrogen-bearing starting materials, as was the case in the studies of Heindl *et al.*[2] and van Hal and Hintzen,[3] but also from the annealing atmosphere, as was also the case in both studies. Our previous work[12] showed that annealing a stoichiometric mixture of CeO_2 (or Ce_2O_3) and SiO_2 in a N_2 atmosphere causes nitrogen to be incorporated into the structure and changes certain *d*-spacings in the diffraction pattern significantly. Although we have not yet studied the effect of the presence of nitrogen on the structure of $Ce_2Si_2O_7$, we suggest that caution be exercised in regard to the purity of the cerium silicates prepared from nitrogen-containing starting materials and nitrogen-bearing annealing atmospheres. Table IV displays the 18 strongest reflections of the XRD pattern of tetragonal $Ce_2Si_2O_7$ prepared from high-purity CeO_2 and fumed SiO_2 in a nitrogen-free atmosphere. The complete XRD pattern of this phase (Table III) can be obtained from the American Ceramic Society depository service.

The polymorphic transformation temperature for $Ce_2Si_2O_7$ was found to be at 1274° ± 3°C. To determine this temperature, we performed four separate DTA runs with 350-mg samples of the tetragonal phase in vacuum ($P_{O_2} \leq 6 \times 10^{-9}$ atm) in Mo crucibles with a heating rate of 1°C/min. Three of these runs consistently produced a small endothermic event at this temperature, as is shown in the sample DTA trace labeled as PYRO 100 in Fig. 1. These three runs were terminated at 1350°C, and the recovered samples were analyzed by XRD. The resultant patterns indicated the presence of the high-temperature monoclinic form of $Ce_2Si_2O_7$. The fourth 350-mg portion of the same tetragonal sample was heated only to 1210°C in the DTA unit and furnace quenched from this temperature. The resultant XRD pattern showed only the tetragonal form of the pyrosilicate.

Calibration of the DTA thermocouples were checked against the Pt melting point and was measured to be at 1772° ± 1°C just prior to the determination of the melting point of $Ce_2Si_2O_7$. We carried out two runs at a heating rate of 3°C/min under vacuum with 320-mg samples of single-phase tetragonal and single-phase monoclinic $Ce_2Si_2O_7$. While the monoclinic sample did not yield any event at the polymorphic transformation temperature, both the tetragonal and monoclinic phases indicated the beginning of melting at temperature 1788° ± 5°C. This temperature correlates well with the previously reported value of 1770° ± 25°C of Toropov *et al.*[6]

In the Al_2O_3–$Ce_2Si_2O_7$ binary, the first 21 compositions of Table II were used for the construction of the phase diagram. After numerous preliminary experiments to determine the required time for the equilibrium phases to form at a given temperature (i.e., 1560°, 1480°, 1400°, and 1300°C), we selected

*For Table III, order ACDS 212 from Data Depository Service, American Ceramic Society, Westerville, OH, 43081.

Table IV. Brief XRD Patterns of Tetragonal and Monoclinic Forms of $Ce_2Si_2O_7$*

Tetragonal $Ce_2Si_2O_7$				Monoclinic $Ce_2Si_2O_7$			
hkl	d_{calc}	d_{obs}	I/I_0	*hkl*	d_{calc}	d_{obs}	I/I_0
101	6.55	6.54	11	110	7.26	7.27	38
110	4.80	4.80	13	200	6.54	6.55	11
112	4.48	4.47	16	021	3.395	3.396	100
113	4.15	4.14	24	−121	3.288	3.289	29
115	3.443	3.441	22	121	3.284	3.283	20
201	3.364	3.365	95	−311	3.168	3.167	10
202	3.274	3.274	70	311	3.158	3.156	6
008	3.087	3.086	100	−320	3.084	3.085	24
211	3.014	3.013	25	−411	2.669	2.669	9
117	2.849	2.848	32	411	2.660	2.659	11
205	2.798	2.797	14	−131	2.515	2.515	10
206	2.619	2.620	12	131	2.513	2.512	8
221	2.390	2.389	13	040	2.182	2.182	10
310	2.148	2.149	12	140	2.152	2.152	13
304	2.125	2.125	18	−322	2.036	2.036	13
314	2.028	2.028	32	−412	2.030	2.030	21
227	1.985	1.985	12	−621	1.837	1.837	10
229	1.807	1.806	12	341	1.834	1.835	10

*Tetragonal $Ce_2Si_2O_7$: a = 6.792 Å, c = 24.700 Å, V = 1139.4 Å^3, Z = 8, SG: $P4_1$ (76). Monoclinic $Ce_2Si_2O_7$: a = 13.080 Å, b = 8.727 Å, c = 5.405 Å, β = 90.13°, Z = 4, V = 617.03 Å^3, SG: $P21/n$ (14).

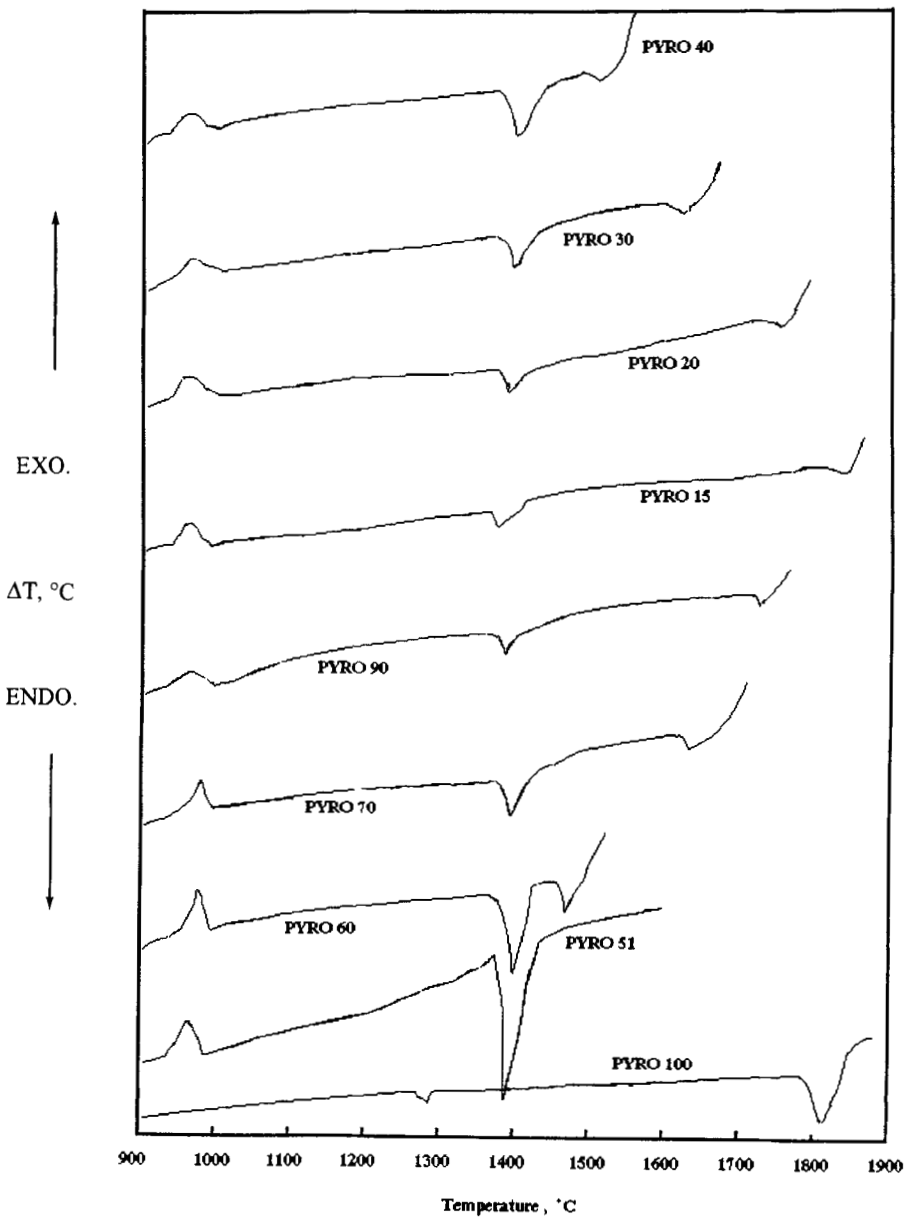

Fig. 1. DTA traces of selected compositions in the Al_2O_3–$Ce_2Si_2O_7$ system.

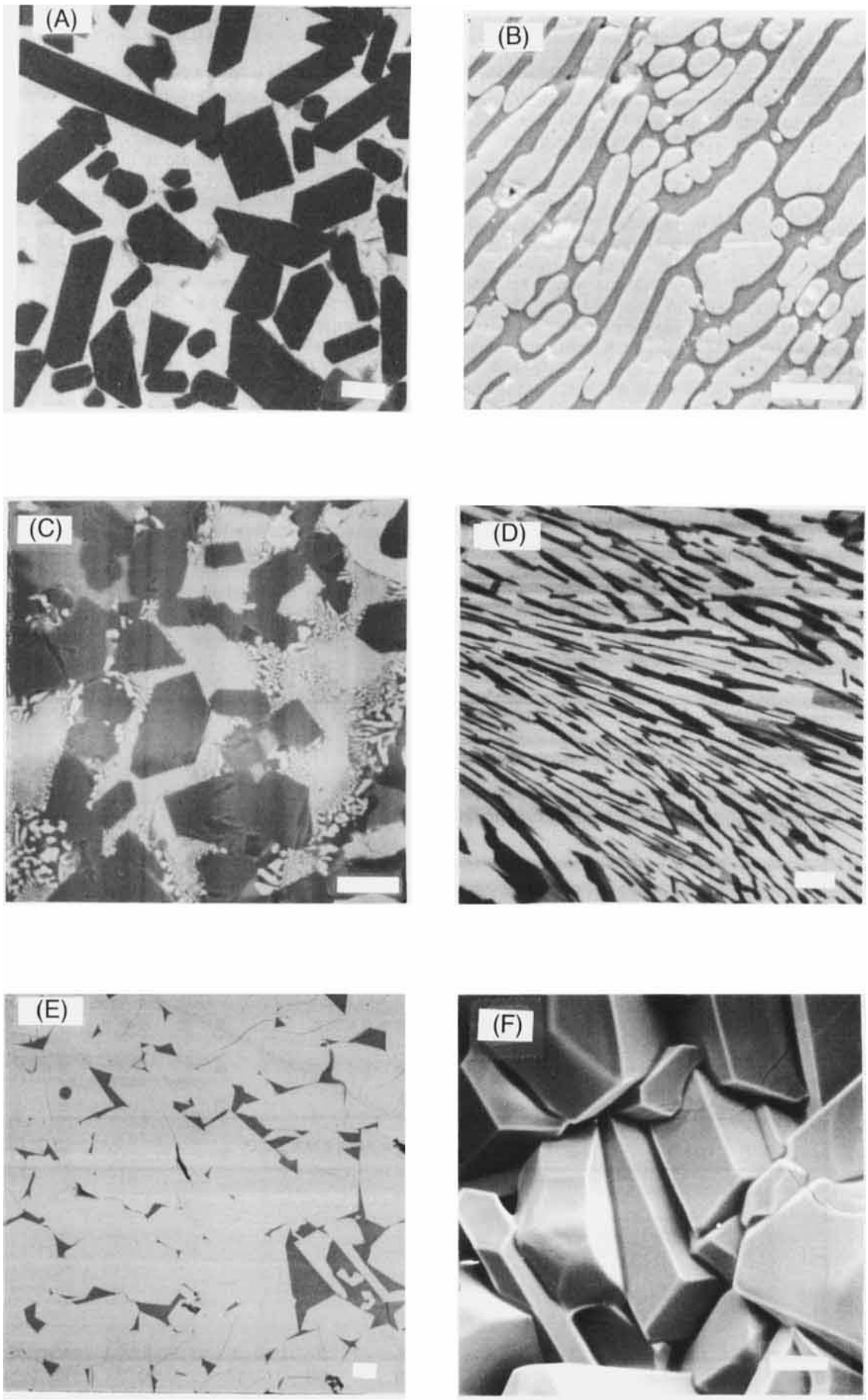

Fig. 2. BSE images of samples in the Al_2O_3–$Ce_2Si_2O_7$ system. (A) Pyro 30: dark alumina grains on a gray once-liquid matrix. (B) Pyro 90: light pyrosilicate streaks on a darker once-liquid matrix. (C) Pyro 15: dark alumina grains, eutectic reaction is continuing. (D) Pyro 51: eutectic microstructure, dark features are alumina. (E) Pyro 95: darker liquid phase between the coarse pyrosilicate grains. (F) Pyro 95: unpolished section; monoclinic pyrosilicate grains are bonded to each other with a darker liquid phase. (Bar lengths = 10 μm.)

the still conservative time of 40 h for 1560°C. All the compositions were annealed at this temperature for 40 h in purified argon and ice-water quenched. Each sample was thoroughly ground and examined with XRD (0.4° 2θ/min, 5°–85° 2θ) to determine the phases present. A small portion of each sample was saved for microstructural analysis by SEM and optical microscopy. The phases observed for this series of samples are summarized in Table II.

The next temperature we chose for the equilibration runs was 1480°C. The five compositions annealed at this temperature (Pyro 15, 30, 50, 70, and 90), produced two solid phases: α-Al_2O_3 and monoclinic $Ce_2Si_2O_7$ as indicated by powder XRD and verified by microscopic analysis. When the equilibration temperature was decreased to 1400°C, the annealing times needed to be increased (as shown in Table II) to form the equilibrium phases. For example, the sample of Pyro 15 composition after annealing at 1400°C for 65 h contained minor amounts of tetragonal $CeAlO_3$ and hexagonal $Ce_2O_3{\cdot}11Al_2O_3$ (cerium hexaaluminate) in addition to the major crystalline α-Al_2O_3 phase. For an annealing time of 85 h at 1400°C, however, the only crystalline phase in the sample was α-Al_2O_3. In the case of Pyro 90 sample (1400°C, 60 h), cerium oxygen apatite ($Ce_{4.67}[SiO_4]_3O$) appeared as a metastable phase, which disappeared upon increasing the annealing time from 60 to 75 h. Reduction in the amount of liquid formed by lowering the annealing temperature slows the reaction kinetics. As a result, longer times are needed for reaching the equilibrium phases.

A backscattered electron (BSE) micrograph of Pyro 30 sample (1400°C, 75 h, quenched) is shown in Fig. 2(A), which displays the α-Al_2O_3 grains dispersed in a liquid matrix which contains Ce, Si, and Al. Figure 2(B), on the other hand, shows the characteristic microstructure of a Pyro 90 sample (1400°C, 75 h, quenched) with the $Ce_2Si_2O_7$ phase dispersed in the darker liquid matrix.

At an annealing temperature of 1300°C, it took over 100 h for the liquid to completely crystallize into α-Al_2O_3 and monoclinic $Ce_2Si_2O_7$ for the Pyro 15 and Pyro 90 compositions, respectively. Figure 2(C) shows the microstructure of a Pyro 15 sample that was first annealed at 1560°C for 40 h and slowly cooled (20°C/h) to 1300°C, where it was annealed for 80 h, and then quenched. It is apparent from this BSE micrograph that the liquid crystallizes primary α-Al_2O_3, followed by the crystallization of the eutectic liquid. It is also observed that the rather sluggish eutectic microstructure formation has been initiated at the most favorable spots in the sample, i.e., at the solid (α-Al_2O_3)–liquid interfaces. Figure 2(D) depicts the BSE micrograph of a sample with the eutectic composition (51 mol% pyrosilicate) first equilibrated at 1560°C and then cooled (35°C/h) to 1300°C, followed by quenching in water. The bright features are monoclinic $Ce_2Si_2O_7$, whereas the dark are α-Al_2O_3. Figure 2(E) displays the BSE micrograph of a Pyro 95 sample where the scarce dark phase is the liquid and the bright phase is monoclinic $Ce_2Si_2O_7$. Figure 2(F) shows an unpolished section of the same sample (Pyro 95) in which the well-crystallized monoclinic $Ce_2Si_2O_7$ grains are cemented together with the darker liquid phase. In this microstructure, Al was found to be confined to the bonding liquid phase.

In order to produce the equilibrium solid-phase mixture below the polymorphic transformation temperature of $Ce_2Si_2O_7$, we annealed the two samples (Pyro 30 and Pyro 75, Table II) in an Ar + 10% H_2 atmosphere in Mo crucibles. These samples were first equilibrated at 1560°C and then slowly

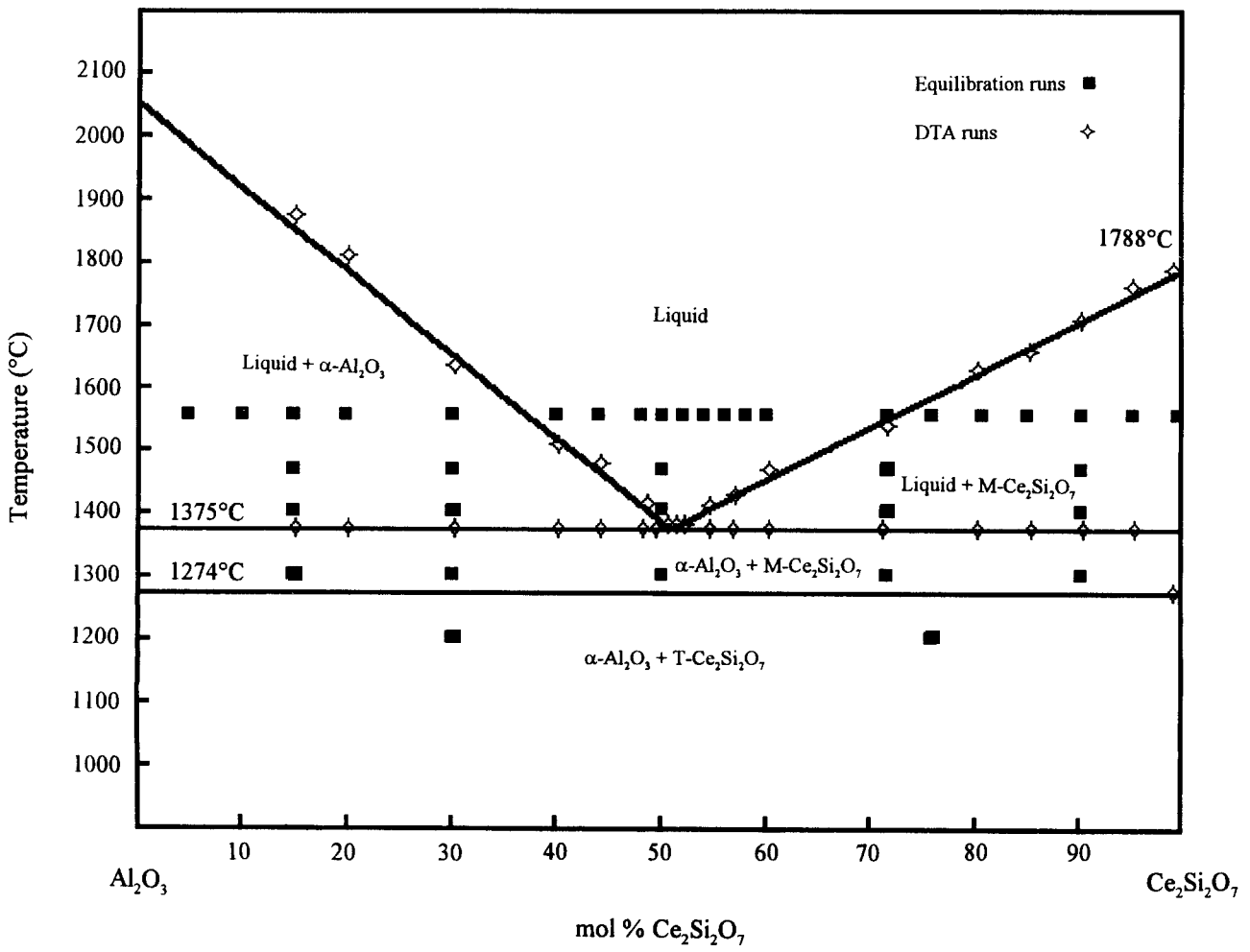

Fig. 3. Binary phase diagram of Al_2O_3–$Ce_2Si_2O_7$ system.

(8°C/h) cooled to 1200°C, followed by 96 h of annealing at that temperature. Although we doubled the cooling rate compared to that employed in the case of pure $Ce_2Si_2O_7$ (to achieve the polymorphic transformation), the presence of the liquid phase helped to improve the transformation kinetics in these samples, and we were able to obtain the solid phases α-Al_2O_3 and tetragonal $Ce_2Si_2O_7$ in the same microstructure.

DTA of the compositions investigated in this study (Table II) was run at both 3°C/min and 6°C/min heating rates in vacuum. Some selected traces from these runs are displayed in Fig. 1. All of the traces shown in this figure represent the heating rate of 3°C/min. The faster DTA scans consistently produced an average of 3°–4°C higher temperatures for the eutectic temperature. The eutectic was found to be at 51 mol% (±0.5 mol%) $Ce_2Si_2O_7$ and a temperature of 1375° ± 5°C. Powder XRD analysis coupled with the DTA experiments indicated that the relatively small exothermic event occurring around 960° ± 30°C, which was common to all of the DTA traces, was due to the formation of crystalline phases from the glassy starting material. For instance, for a sample of Pyro 30, that peak corresponded to the crystallization of $Ce_2Si_2O_7$, as indicated by the XRD analysis of a sample recovered from a DTA run which was terminated at 1025°C, whereas, for a sample of Pyro 70 composition, this peak belonged to the crystallization of α-Al_2O_3. For all the DTA traces shown in Fig. 1, the second, endothermic event indicated the first liquid formation in the system, while the third thermal event (if there was one) represented the disappearance of the solid phase completely. The rather drastic change observed in the slope of the DTA lines at and beyond this point, preceded by a significant endothermic-like disturbance to the baseline, indicated the presence of a rising/crawling up liquid along the inner walls, eventually emptying the inside of the sample pan. Upon the prevalence of this condition, the thermal balance between the sample and the reference pans (which had dictated the slope of the baseline until that point) had been lost, and the baseline began to display a sharp rise with increasing temperature. Based on the phase information gathered from the equilibration runs and the DTA data, the binary phase diagram of Al_2O_3–$Ce_2Si_2O_7$ shown in Fig. 3 was constructed. The phase diagram displays a simple eutectic reaction with a polymorphic transformation in $Ce_2Si_2O_7$ below the eutectic temperature.

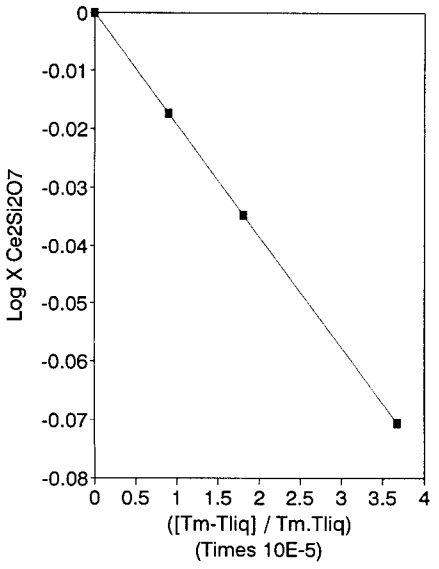

Fig. 4. Heat of melting of $Ce_2Si_2O_7$ calculated from the slope of its liquidus line.

Assuming ideal mixing in the liquid phase and complete immiscibility of α-Al_2O_3 in solid $Ce_2Si_2O_7$, the enthalpy of the melting of $Ce_2Si_2O_7$ can be calculated from the experimentally determined liquidus line, using the freezing point depression of $Ce_2Si_2O_7$ by the addition of Al_2O_3, according to

$$\log X_A = -\frac{\Delta H_{m,A}}{R}\left[\frac{(T_{m,A} - T_L)}{T_{m,A}T_L}\right] \quad (1)$$

where $A = Ce_2Si_2O_7$. Therefore, a plot of $\log X_{Ce_2Si_2O_7}$ (liquidus) against the term $[(T_{m,Ce_2Si_2O_7} - T_{liquidus})/T_{m,Ce_2Si_2O_7}T_{liquidus}]$ should be a straight line with a slope equal to $(-\Delta H^\circ_{m,Ce_2Si_2O_7}/2.303R)$. The plot of this line is given in Fig. 4, from which we calculated $\Delta H^\circ_{m,Ce_2Si_2O_7}$ to be 36.81 ± 0.25 kJ/mol. This translates to a value for $\Delta S^\circ_{m,Ce_2Si_2O_7}$ of 17.86 J/mol·K at the melting point of 1788°C. No values were found in the literature for the enthalpy and entropy of melting of any of the lanthanide pyrosilicates to compare with these data.

IV. Conclusions

(1) It was found that cerium pyrosilicate, $Ce_2Si_2O_7$, like other light lanthanide pyrosilicates has two polymorphic forms. The high-temperature form is monoclinic and the low-temperature form is tetragonal. The low-temperature, tetragonal polymorph of $Ce_2Si_2O_7$ can be produced only by slowly cooling the high-temperature form if the high-temperature form had been prepared from pure binary oxides, CeO_2 and SiO_2 in an inert atmosphere. The polymorphic transformation occurs at 1274° ± 5°C. The melting point of $Ce_2Si_2O_7$ was determined to be 1788° ± 5°C using DTA experiments.

(2) The Al_2O_3–$Ce_2Si_2O_7$ binary system is of the simple eutectic type. The eutectic occurs at 1375° ± 5°C and 51 mol% $Ce_2Si_2O_7$. The enthalpy of melting of the cerium pyrosilicate phase was calculated as 36.81 kJ/mol from the slope of the liquidus.

(3) The microstructures in this binary system can be controlled by proper selection of heating and cooling rates and annealing times. The equilibrium phases formed and depicted here require a strict control over the inertness of the annealing atmosphere.

References

[1]J. Felsche, "Polymorphism and Crystal Data of the Rare-Earth Disilicates of Type $RE_2Si_2O_7$," *J. Less-Common Met.*, **21**, 1–14 (1970).

[2]R. Heindl, N. Jonkierre, and J. A. Loriers, "Preparation and Luminescence Properties of Tetragonal Cerium Disilicate $Ce_2Si_2O_7$ and Its Terbium-Activated Derivative," *Proc. Rare Earth Res. Conf., 9th*, **1**, 25–34 (1971).

[3]H. A. M. van Hal and H. T. Hintzen, "Compound Formation in the Ce_2O_3–SiO_2 System," *J. Alloys Compd.*, **179**, 77–85 (1992).

[4]J. Felsche and W. Hirsiger, "The Polymorphs of the Rare-Earth Pyrosilicates $RE_2Si_2O_7$," *J. Less-Common Met.*, **18**, 131 (1969).

[5]C. Calvo, "The Crystal Structure of α-$Ca_2P_2O_7$," *Inorg. Chem.*, **7**, 1345–51 (1968).

[6]N. A. Toropov, I. F. Andreev, A. N. Sokolov, and L. N. Sanzharevskaya, "Solid Solutions in the System $Y_2Si_2O_7$–$Ce_2Si_2O_7$," *Izv. Akad. Nauk SSSR, Neorg. Mater.*, **6** [3] 519–23 (1970).

[7]A. I. Leonov, "The Valence of Cerium in Synthetic and Natural Cerium Aluminates and Silicates, Part 2, Cerium Silicates," *Izv. Akad. Nauk SSSR, Ser. Khim.*, **12**, 2084–89 (1963).

[8]M. H. O'Brien and M. Akinc, "Role of Ceria in Enhancing the Resistance of Aluminosilicate Refractories to Attack by Molten Aluminum Alloy," *J. Am. Ceram. Soc.*, **72** [6] 896–904 (1989).

[9]E. I. Galant and V. A. Tsekhomskii, "The Electron Conductivity of Cerium-Containing Glasses," *Izv. Akad. Nauk SSSR, Neorg. Mater.*, **3** [10] 1953–55 (1967).

[10]A. Makishima, M. Kobayashi, T. Shimohira, and T. Nagata, "Formation of Aluminosilicate Glasses Containing Rare-Earth Oxides," *J. Am. Ceram. Soc.*, **65** [12] C-210 (1982).

[11]E. M. Levin, C. R. Robbins and H. F. McMurdie, *Phase Diagrams for Ceramists*; Fig. 356. Edited by M. K. Reser. American Ceramic Society, Columbus, OH, 1964.

[12]A. C. Tas and M. Akinc, "Cerium Oxygen Apatite ($Ce_{4.67}[SiO_4]_3O$) X-ray Diffraction Pattern Revisited," *Powder Diffr.*, **7**, 219–22, 1992.